

ELECTRON–PHONON INTERACTION AND COUPLED PHONON–PLASMON MODES

*L. A. Falkovsky**

*Landau Institute for Theoretical Physics
117337, Moscow, Russia*

Submitted 24 March 2003

The theory of Raman scattering by the coupled electron–phonon system in metals and heavily doped semiconductors is developed with the Coulomb screening and the electron–phonon deformation interaction taken into account. The Boltzmann equation for carriers is applied. Phonon frequencies and optic coupling constants are renormalized due to interactions with carriers. The k -dependent semiclassical dielectric function is involved instead of the Lindhard–Mermin expression. The results of calculations are presented for various values of the carrier concentration and the electron–phonon coupling constant.

PACS: 63.20.Dj, 63.20.Kr, 71.38.-k, 72.30.+q, 78.30.-j

1. INTRODUCTION

Recently, there has been considerable interest in the effect of electron–phonon interactions on the optical-phonon dispersion. This interest is stimulated by contradictions between different approaches to the electron–phonon interaction. The strong phonon renormalizations were first obtained by Migdal [1] (see also [2]) within a consistent many-body approach based on the Fröhlich Hamiltonian. The extremely large dispersion of optical phonons was predicted in [3] also using the Fröhlich model. These results contradict Born–Oppenheimer (adiabatic) concept [4] according to which the phonon renormalizations should be small in terms of the nonadiabatic parameter $\sqrt{m/M}$, where m and M are the electron and ion masses, respectively (see also [5]). Theoretical investigations [6] of the sound velocity and acoustic attenuation in metals confirm the adiabatic concept. In a recent paper, Reizer [7] emphasized the importance of taking the screening effect into account. To our knowledge, the Coulomb screening effect on LO phonons was first studied in [8]. Using the Boltzmann equation, we found in [9] that the electron–phonon interaction results more considerably in the optical–phonon damping than in the dispersion law. In any case, the Fröhlich model has the evident shortcomings.

From the experimental standpoint, the best opportunity for the investigation of interactions between electrons and optical phonons is provided by coupled phonon–plasmon modes in doped semiconductors (see, e.g., [10]). Two such modes, L^\pm , have been observed in Raman experiments for many semiconductors. At the early stage, the Raman results were compared with the theory [11] based on the Drude model (see, e.g., [12]), but the Lindhard–Mermin expression for the dielectric function was used more recently [13].

The Lindhard–Mermin expression [14] represents a sophisticated generalization of the Lindhard function with the help of the electron relaxation time. The Lindhard approach is very useful while the momentum transfer k in the Raman scattering is compared with the Fermi momentum p_F . The most significant effect of the carriers should be expected for $kv_F \sim \omega$, where v_F is the Fermi velocity and ω is the phonon frequency. For solids with metallic conductivity, the Fermi velocity can be estimated using the argument of stability under the Coulomb interaction $e^2/\pi\hbar v_F \leq 1$. This condition gives $v_F \sim 0.7 \cdot 10^8$ cm/s. For the typical value of the optical phonon frequency $\omega = 500$ cm⁻¹, the interesting values are $k \leq \omega/v_F \approx 10^6$ cm⁻¹. Therefore, the condition $k < p_F$ is satisfied for the carrier concentration larger than $3 \cdot 10^{17}$ cm⁻³. In experiments, the heavily doped semiconductors with large carrier concentration are used in order to obtain a visible effect of carriers. The condition $k \ll p_F$ is then satisfied,

*E-mail: falk@itp.ac.ru

and we can apply the Boltzmann equation in calculations of the electronic susceptibility and in the evaluation of the Raman cross section. The method of the Boltzmann equation is valid for the anisotropic electron plasma in solids at arbitrary temperatures. In the present paper, we obtain the Raman efficiency applying the Boltzmann equation for generate carriers in heavily doped semiconductors at the temperature lower than the Fermi energy, $T \ll \varepsilon_F$.

2. EFFECTIVE HAMILTONIAN AND LIGHT SCATTERING

For the electron–phonon system in solids, we use the operator of particle numbers \hat{n} , the phonon displacements \hat{b}_j , and the macroscopic electric field E that accompanies vibrations in polar semiconductors and acts on the electron and ion charges. The effective Hamiltonian describing the inelastic light scattering in solids can be written in the semiclassical Wigner representation as

$$\mathcal{H} = \frac{e^2}{mc^2} \int d^3r \mathcal{N}(\mathbf{r}, t) U(\mathbf{r}, t), \tag{1}$$

where

$$\mathcal{N}(\mathbf{r}, t) = \gamma \hat{n}(\mathbf{r}, t) + g_j \hat{b}_j(\mathbf{r}, t) + g_E E(\mathbf{r}, t) \tag{2}$$

is a linear form in the variables \hat{n} , \hat{b}_j , and E . The subscript « j » denotes the various phonon modes, longitudinal (LO) or transverse (TO). More precisely, the subscript « j » labels the different phonon representations, which can be degenerate. The transformation properties of the coupling constants g_j are determined by this representation. The notation $U(\mathbf{r}, t)$ is introduced for a product of the vector potentials of the incident and scattered photons,

$$A^{(i)}(\mathbf{r}, t) A^{(s)}(\mathbf{r}, t) = U(\mathbf{r}, t) = \exp[i(\mathbf{k} \cdot \mathbf{r} - \omega t)] U(\mathbf{k}, \omega),$$

where the momentum and frequency transfers are $\mathbf{k} = \mathbf{k}^{(i)} - \mathbf{k}^{(s)}$ and $\omega = \omega^{(i)} - \omega^{(s)}$. The polarization vectors of $\hat{\mathbf{b}}_j(\mathbf{r}, t)$, $\mathbf{E}(\mathbf{r}, t)$, $\mathbf{A}^{(i)}(\mathbf{r}, t)$, and $\mathbf{A}^{(s)}(\mathbf{r}, t)$ are included in the coupling constants.

The first term in the right-hand side of Eq. (2) describes the light scattering by electron–hole pairs with the vertex

$$\gamma(\mathbf{p}) = e_\alpha^{(i)} e_\beta^{(s)} \left[\delta_{\alpha\beta} + \frac{1}{m} \times \sum_n \left(\frac{p_{fn}^\beta p_{nf}^\alpha}{\varepsilon_f(\mathbf{p}) - \varepsilon_n(\mathbf{p}) + \omega^{(i)}} + \frac{p_{fn}^\beta p_{nf}^\alpha}{\varepsilon_f(\mathbf{p}) - \varepsilon_n(\mathbf{p}) - \omega^{(s)}} \right) \right],$$

where the resonant term is included; $e_\alpha^{(i)}$ and $e_\beta^{(s)}$ are the polarization vectors of the incident, $\mathbf{A}^{(i)}(\mathbf{r}, t)$, and scattered, $\mathbf{A}^{(s)}(\mathbf{r}, t)$, photons. The quantum-mechanical and statistical average of the first term in Eq. (2),

$$\langle\langle \gamma \hat{n}(\mathbf{r}, t) \rangle\rangle = \int \frac{2d^3p}{(2\pi)^3} \gamma(\mathbf{p}) f_p(\mathbf{r}, t), \tag{3}$$

can be expressed in terms of the electron distribution function $f_p(\mathbf{r}, t)$. The constants g_j and g_E are the deformation-optic and electro-optic couplings with the phonon displacements and the macroscopic electric field, respectively. The estimation gives $g_j \sim 1/a^4$, $g_E \sim 1/ea$, and $\gamma(\mathbf{p}) \sim m/m^*$, where a is the lattice parameter and m^* is the effective mass.

The variable $U(\mathbf{r}, t)$ can be considered as an external force. The generalized susceptibility $\chi(\mathbf{k}, \omega)$ is then introduced as the linear response to this force,

$$\langle\langle \mathcal{N}(\mathbf{k}, \omega) \rangle\rangle = -\chi(\mathbf{k}, \omega) U(\mathbf{k}, \omega). \tag{4}$$

According to the fluctuation–dissipation theorem, the function

$$K(\mathbf{k}, \omega) = \frac{2}{1 - e^{-\omega/T}} \text{Im} \chi(\mathbf{k}, \omega)$$

is the Fourier component of the correlation function

$$K(\mathbf{r}, t; \mathbf{r}', t') = \langle\langle \mathcal{N}^\dagger(\mathbf{r}, t) \mathcal{N}(\mathbf{r}', t') \rangle\rangle \tag{5}$$

that depends only on the differences $\mathbf{r} - \mathbf{r}'$ and $t - t'$. The Raman cross section is given by

$$\frac{d\sigma}{d\omega^{(s)} d\Omega^{(s)}} = \frac{k_z^{(s)} \omega^{(s)}}{\pi c} \left(\frac{2e^2}{\hbar m \omega^{(i)}} \right)^2 K(\mathbf{k}, \omega) |U(\mathbf{k}, \omega)|^2, \tag{6}$$

where $k_z^{(s)}$ is the normal to the sample surface component of the scattered wave vector in vacuum.

A note should be made. Evidently, any sample has the surface. The surface effects in the Raman scattering were considered in our paper [15]; they are omitted in the derivation of Eq. (6). Because of the skin effect, the incident and scattered fields do not penetrate the bulk. For the optical range of the incident light, we have the normal skin-effect conditions. We then integrate the distribution $|U(\mathbf{k}, \omega)|^2$ in Eq. (6) over the normal component k_z . As shown in [15], the integration of $|U(\mathbf{k}, \omega)|^2$ gives the factor $1/\zeta_2$, where ζ_2 is expressed in terms of the wave-vector components inside the semiconductor, $\zeta_2 = \text{Im}(k_z^{(i)} + k_z^{(s)})$. The Raman cross section (6) is dimensionless. It represents the ratio of the inelastic scattered light energy to the incident energy.

3. BOLTZMANN EQUATION FOR CARRIERS

The problem of the evaluation of the Raman cross section consists in the calculation of generalized susceptibility (4). We apply the Boltzmann equation for the electron distribution function:

$$\frac{\partial f_p(\mathbf{r}, t)}{\partial t} + \mathbf{v} \frac{\partial f_p(\mathbf{r}, t)}{\partial \mathbf{r}} + \dot{\mathbf{p}} \frac{\partial f_p(\mathbf{r}, t)}{\partial \mathbf{p}} = -\frac{1}{\tau} [f_p(\mathbf{r}, t) - \langle f_p(\mathbf{r}, t) \rangle]. \quad (7)$$

The angular brackets denote the average over the Fermi surface,

$$\langle \dots \rangle = \frac{1}{\nu_0} \int (\dots) \frac{2dS_F}{v(2\pi)^3},$$

where the integral is performed in the momentum space over the Fermi surface and ν_0 is the density of electron states, defined by the condition $\langle 1 \rangle = 1$. We use the τ -approximation, which is correct for the electron scattering by defects and phonons at room temperatures. The collision integral in form (7) conserves the number of electrons in collisions. Therefore, the charge density satisfies the equation of continuity. This ensures the correct ω -dependence of the dielectric function at low frequencies.

In accordance with Eqs. (1), (2), and (3), instead of the unperturbed electron spectrum $\varepsilon_0(\mathbf{p})$, we introduce the local electron spectrum in the presence of the external force $U(\mathbf{r}, t)$ as

$$\varepsilon(\mathbf{p}, \mathbf{r}, t) = \varepsilon_0(\mathbf{p}) + \gamma(\mathbf{p})U(\mathbf{r}, t) + \zeta_j(\mathbf{p})b_j(\mathbf{r}, t),$$

where the last term represents the electron–optical-phonon deformation potential and $b_j(\mathbf{r}, t) = \langle \hat{b}_j(\mathbf{r}, t) \rangle$. We use this form of the electron–phonon interaction instead of the polarization type interaction $\zeta(\mathbf{p})\text{div}\mathbf{b}(\mathbf{r}, t)$ (see [9]) because the first is larger by the parameter $1/ka$ for the optical phonons.

We linearize Eq. (7), seeking its solution in the form

$$f_p(\mathbf{r}, t) = f_0[\varepsilon(\mathbf{p}, \mathbf{r}, t) - \mu] - \frac{df_0}{d\varepsilon} \delta f_p(\mathbf{r}, t), \quad (8)$$

where $f_0[\varepsilon(\mathbf{p}, \mathbf{r}, t) - \mu]$ is the Fermi–Dirac local distribution function. It is important that the collision term in the Boltzmann equation is canceled if this local distribution function is only used.

We impose the number conservation condition on the chemical potential,

$$\int \frac{d^3p}{(2\pi)^3} f_0[\varepsilon(\mathbf{p}, \mathbf{r}, t) - \mu] = \int \frac{d^3p}{(2\pi)^3} f_0(\varepsilon_0 - \mu_0),$$

and obtain

$$\mu = \mu_0 + \langle \gamma(\mathbf{p}) \rangle U(\mathbf{r}, t) + \langle \zeta_j(\mathbf{p}) \rangle b_j(\mathbf{r}, t).$$

The condition implies the renormalization of vertices

$$\gamma(\mathbf{p}) \rightarrow \gamma(\mathbf{p}) - \langle \gamma(\mathbf{p}) \rangle, \quad \zeta_j(\mathbf{p}) \rightarrow \zeta_j(\mathbf{p}) - \langle \zeta_j(\mathbf{p}) \rangle, \quad (9)$$

and this substitution is to be made in what follows.

The linearized Boltzmann equation in the Fourier components is given by

$$-i(\omega - \mathbf{k} \cdot \mathbf{v} + i/\tau) \delta f_p(\mathbf{k}, \omega) = \psi_p(\mathbf{k}, \omega) + \langle \delta f_p(\mathbf{k}, \omega) \rangle / \tau,$$

where

$$\psi_p(\mathbf{k}, \omega) = e\mathbf{v} \cdot \mathbf{E}(\mathbf{k}, \omega) - i\omega[\gamma(\mathbf{p})U(\mathbf{k}, \omega) + \zeta_j(\mathbf{p})b_j(\mathbf{k}, \omega)].$$

The solution to this equation is easily obtained as

$$\delta f_p(\mathbf{k}, \omega) = i[\psi_p(\mathbf{k}, \omega) + \langle \delta f_p(\mathbf{k}, \omega) \rangle / \tau] / \Delta_p, \quad (10)$$

where we designate $\Delta_p = \omega - \mathbf{k} \cdot \mathbf{v} + i/\tau$. We now obtain

$$\langle \delta f_p(\mathbf{k}, \omega) \rangle = \frac{i\langle \psi_p(\mathbf{k}, \omega) / \Delta_p \rangle}{1 - i\langle \tau^{-1} / \Delta_p \rangle}. \quad (11)$$

Notice that in accordance with the adiabatic concept, no additional contribution comes from the local equilibrium distribution function $f_0[\varepsilon(\mathbf{p}, \mathbf{r}, t)]$ in Eq. (8).

4. EQUATION OF MOTION FOR PHONONS INTERACTING WITH CARRIERS

In the long-wave approximation ($k \ll 1/a$, where a is the lattice parameter), we write the equation of motion for the phonon displacement field as

$$(\omega_k^2 - \omega^2)b_j(\mathbf{k}, \omega) = \frac{Z}{M'} E_j(\mathbf{k}, \omega) - \frac{g_j U(\mathbf{k}, \omega)}{M'N} - \frac{1}{M'N} \int \frac{2dS_F}{v(2\pi)^3} \zeta_j(\mathbf{p}) \delta f_p(\mathbf{k}, \omega), \quad (12)$$

where N is the number of unit cells in 1 cm^3 , M' is the reduced mass of the unit cell, and Z is the effective ionic charge. The nonperturbed phonon frequency ω_k must be considered in the absence of the electric field and without any electron–phonon interactions. In the long-wave limit, we can expand it as $\omega_k^2 = \omega_0^2 \pm s^2 k^2$ with the value of the dispersion parameter s of the order of the typical sound velocity in solids. We note that the optical phonons always have the so-called natural width $\Gamma^{nat} \sim \omega_0 \sqrt{m/M}$. The natural width results from decay processes into two or more acoustic and optical phonons. In the final expressions, we will substitute $\omega_k^2 - \omega^2 \rightarrow \omega_k^2 - i\omega\Gamma^{nat} - \omega^2$.

Equation (12) is applied to both the longitudinal and transverse phonons. It follows from the Maxwell equations that the electric field is longitudinal, $\mathbf{E} \parallel \mathbf{k}$, in the optical region $k \gg \omega/c$. If the excited phonons propagate in the symmetric direction, the TO and LO phonons are separated. Therefore, the electric field is involved only in Eq. (12) for the LO phonon. In addition, the coupling $\zeta_j(\mathbf{p})$ depends on the phonon representation j .

Using solution (10), we rewrite Eq. (12) as

$$(\tilde{\omega}_j^2 - \omega^2)b_j(\mathbf{k}, \omega) - \frac{\tilde{Z}}{M'}E_j(\mathbf{k}, \omega) = -\frac{\tilde{g}_j U(\mathbf{k}, \omega)}{M'N}, \quad (13)$$

where the phonon frequency

$$\tilde{\omega}_j^2 = \omega_k^2 + \frac{\omega\nu_0}{M'N} \left(\left\langle \frac{\zeta_j^2(\mathbf{p})}{\Delta_p} \right\rangle + \frac{i\langle \zeta_j(\mathbf{p})/\Delta_p \rangle^2}{\tau - \langle i/\Delta_p \rangle} \right), \quad (14)$$

the effective ionic charge

$$\tilde{Z} = Z - \frac{ie\nu_0}{N} \left(\left\langle \frac{v_z \zeta_j(\mathbf{p})}{\Delta_p} \right\rangle + \frac{i\langle v_z/\Delta_p \rangle \langle \zeta_j(\mathbf{p})/\Delta_p \rangle}{\tau - \langle i/\Delta_p \rangle} \right), \quad (15)$$

and the deformation–optic coupling

$$\tilde{g}_j = g_j + \omega\nu_0 \left(\left\langle \frac{\zeta_j(\mathbf{p})\gamma(\mathbf{p})}{\Delta_p} \right\rangle + \frac{i\langle \zeta_j(\mathbf{p})/\Delta_p \rangle \langle \gamma(\mathbf{p})/\Delta_p \rangle}{\tau - \langle i/\Delta_p \rangle} \right) \quad (16)$$

are renormalized because of the electron–phonon interaction $\zeta_j(\mathbf{p})$.

5. POISSON EQUATION FOR THE MACROSCOPIC FIELD

We consider the longitudinal electric induction D that accompanies lattice vibrations. There are several contributions to the field: (1) the polarization $\alpha E(\mathbf{r}, t)$ of the filled electron bands; (2) the lattice polarization $NZb_{LO}(\mathbf{r}, t)$; (3) the contribution of the free carrier density $\rho = -\text{div} \mathbf{P}_e$; and (4) the term $P = -\partial\mathcal{H}/\partial E = -g_E U$ that explicitly results from Hamiltonian (1), (2). Collecting all these terms into the Poisson equation $\text{div} \mathbf{D} = 0$ we find

$$\varepsilon_\infty E(\mathbf{k}, \omega) + 4\pi N Z b_{LO}(\mathbf{k}, \omega) + \frac{4\pi ie}{k} \int \frac{2d^3p}{(2\pi)^3} \delta f_p(\mathbf{k}, \omega) - 4\pi g_E U(\mathbf{k}, \omega) = 0, \quad (17)$$

where the high-frequency permittivity $\varepsilon_\infty = 1 + 4\pi\alpha$. Using the solution of the Boltzmann equation, we rewrite the Poisson equation in the form

$$\varepsilon_e(\mathbf{k}, \omega)E(\mathbf{k}, \omega) + 4\pi N \bar{Z} b_{LO}(\mathbf{k}, \omega) = 4\pi \tilde{g}_E U(\mathbf{k}, \omega), \quad (18)$$

where the electronic dielectric function

$$\varepsilon_e(\mathbf{k}, \omega) = \varepsilon_\infty + \varepsilon_\infty \frac{k_0^2}{k^2} \left[1 - \frac{\langle \omega/\Delta_p(k) \rangle}{1 - \langle i/\Delta_p(k) \rangle/\tau} \right] \quad (19)$$

contains the Thomas–Fermi parameter $k_0^2 = 4\pi e^2 \nu_0 / \varepsilon_\infty$.

Because of the electron–phonon interactions $\zeta_{LO}(\mathbf{p})$, the ionic charge obtains an additional term,

$$\bar{Z} = Z + \frac{ie\nu_0}{N} \times \left(\left\langle \frac{v_z \zeta_{LO}(\mathbf{p})}{\Delta_p} \right\rangle + \frac{i\langle v_z/\Delta_p \rangle \langle \zeta_{LO}(\mathbf{p})/\Delta_p \rangle}{\tau - \langle i/\Delta_p \rangle} \right), \quad (20)$$

of the opposite sign compared with that in Eq. (15). The electro-optic coupling in Eq. (17) also changes, but because of the light scattering by carriers $\gamma(\mathbf{p})$:

$$\tilde{g}_E = g_E - ie\nu_0 \left(\left\langle \frac{v_z \gamma(\mathbf{p})}{\Delta_p} \right\rangle + \frac{i\langle v_z/\Delta_p \rangle \langle \gamma(\mathbf{p})/\Delta_p \rangle}{\tau - \langle i/\Delta_p \rangle} \right). \quad (21)$$

6. RAMAN SCATTERING BY ELECTRON–HOLE PAIRS, PHONONS, AND COUPLED MODES

We are now in a position to calculate susceptibility (4). Using Eqs. (3), (10), (11), (16), and (21), we obtain

$$\langle \langle \mathcal{N}(\mathbf{k}, \omega) \rangle \rangle = -\chi_e(\mathbf{k}, \omega)U(\mathbf{k}, \omega) + \tilde{g}_j b_j(\mathbf{k}, \omega) + \bar{g}_E E(\mathbf{k}, \omega), \quad (22)$$

where

$$\chi_e(\mathbf{k}, \omega) = -\omega\nu_0 \left(\left\langle \frac{\gamma^2(\mathbf{p})}{\Delta_p} \right\rangle + \frac{i\langle \gamma(\mathbf{p})/\Delta_p \rangle^2}{\tau - \langle i/\Delta_p \rangle} \right)$$

gives the light scattering with the excitation of electron–hole pairs. We note that the renormalized coupling \bar{g}_E entering here differs from \tilde{g}_E in (21) by the sign of the second term:

$$\bar{g}_E = g_E + ie\nu_0 \left(\left\langle \frac{v_z \gamma(\mathbf{p})}{\Delta_p} \right\rangle + \frac{i\langle v_z/\Delta_p \rangle \langle \gamma(\mathbf{p})/\Delta_p \rangle}{\tau - \langle i/\Delta_p \rangle} \right).$$

To find $E(\mathbf{k}, \omega)$ and $b_j(\mathbf{k}, \omega)$, we must solve the system of algebraic equations (13) and (18). Using Eq. (22), we then obtain the generalized susceptibility

$$\chi(\mathbf{k}, \omega) = \chi_e(\mathbf{k}, \omega) + \frac{\tilde{g}_j^2 \varepsilon_e(\mathbf{k}, \omega)/NM' - 4\pi\tilde{g}_E\bar{g}_E(\tilde{\omega}_j^2 - \omega^2) - 4\pi\tilde{g}_j(\tilde{g}_E\tilde{Z} + \bar{g}_E\bar{Z})/M'}{(\tilde{\omega}_j^2 - \omega^2)\varepsilon_e(\mathbf{k}, \omega) + 4\pi N\tilde{Z}\bar{Z}/M'}. \quad (23)$$

Expression (23) is our main result. The poles of the second term give the spectrum of collective excitations of the electron-phonon system. We discuss Eq. (23) in various limiting cases.

6.1. The electronic scattering

We obtain the Raman electronic scattering from Eq. (23) if we set $\tilde{g}_j = g_E = \tilde{Z} = \bar{Z} = 0$. We then have

$$\chi(\mathbf{k}, \omega) = \chi_e(\mathbf{k}, \omega) + \frac{4\pi\tilde{g}_E^2}{\varepsilon_e(\mathbf{k}, \omega)}, \quad (24)$$

where \tilde{g}_E is given by Eq. (21) with $g_E = 0$.

For the isotropic Fermi surface, we calculate the dielectric function in Eq. (19) by performing the integration:

$$\left\langle \frac{1}{\Delta_p(k)} \right\rangle = \frac{1}{2kv_F} \ln \frac{1+\kappa}{1-\kappa}, \quad \kappa = \frac{kv_F}{\omega + i\tau^{-1}}, \quad (25)$$

where we must take the branch of $\ln x$ that is real for positive real values of x .

For the anisotropic Fermi surface, the calculations can be done in limiting cases. For $|\kappa| \gg 1$, we use the expansion for electronic dielectric function (19),

$$\begin{aligned} \varepsilon_e(\mathbf{k}, \omega) &= \\ &= \varepsilon_\infty \left\{ 1 + \left(\frac{k_0}{k} \right)^2 \left[1 + i \frac{\pi\nu_0\omega}{k} \left\langle \frac{1}{v} \delta(\mu) \right\rangle \right] \right\}, \quad (26) \end{aligned}$$

where $\mu = \mathbf{v} \cdot \mathbf{k}/vk$ and $\delta(x)$ is the Dirac delta function. In this case, the Raman efficiency has a «tail» due to the Landau damping,

$$\text{Im } \chi(\mathbf{k}, \omega) = \frac{\pi\nu_0\omega}{k} \left\langle \frac{\gamma^2(\mathbf{p})}{v} \delta(\mu) \right\rangle. \quad (27)$$

We see that the Raman cross section vanishes for the isotropic vertex $\gamma(\mathbf{p})$ because of Eq. (9). This is a result of the Coulomb screening. It was first obtained in [16] for the Raman scattering in semiconductors (see [17]).

In the opposite case where $|\kappa| \ll 1$, the first term in Eq. (24) gives the result

$$\text{Im } \chi_e(\mathbf{k}, \omega) = \nu_0 \langle \gamma^2(\mathbf{p}) \rangle \frac{\omega\tau}{(\omega\tau)^2 + 1}, \quad (28)$$

which was first found in [18] with the help of the Green's function technique. The second term in Eq. (24) reveals a plasmon pole at small values of k . The k -expansion of the dielectric function reads

$$\varepsilon_e(k, \omega) = \varepsilon_\infty \left(1 - \frac{\omega_{pe}^2 + k^2 w}{\omega(\omega + i\tau^{-1})} \right), \quad (29)$$

where the k -independent term represents the Drude conductivity and the electron plasma frequency is given by the integral over the Fermi surface, $\omega_{pe}^2 = k_0^2 \langle v_z^2 \rangle$. The complex coefficient

$$w = \frac{k_0^2 (\langle v_z^4 \rangle + i \langle v_z^2 \rangle^2 / \omega\tau)}{(\omega + i\tau^{-1})^2}.$$

For the quadratic electron spectrum, $\langle v_z^2 \rangle = v_F^2/3$ and $\langle v_z^4 \rangle = v_F^4/5$.

The k -expansion of \tilde{g}_E gives

$$\tilde{g}_E = -\frac{ie\nu_0 k \langle \gamma(\mathbf{p}) v_z^2 \rangle}{(\omega + i\tau^{-1})^2}$$

because $g_E = 0$ and the zero-order term in the k -expansion vanishes due to the time invariance $\mathbf{v} \rightarrow -\mathbf{v}$. The intensity of the plasmon peak is then proportional to k^2 , in accordance with the known behavior of the dynamical structure factor.

6.2. The Raman scattering by TO phonons

The second term in Eq. (23) gives the TO-phonon scattering if we set $\tilde{Z} = \bar{Z} = \tilde{g}_E = 0$:

$$\chi(\mathbf{k}, \omega) = \frac{\tilde{g}_{TO}^2 / NM'}{\tilde{\omega}_{TO}^2 - \omega^2 - i\omega\Gamma^{nat}}, \quad (30)$$

where $\tilde{\omega}_{TO}$ and \tilde{g}_{TO} are defined in Eqs. (14) and (16) with $\zeta_j(\mathbf{p}) = \zeta_{TO}(\mathbf{p})$; we add the phonon width Γ^{nat} mentioned above.

Two points must be noted here. First, the TO-resonance occurs at the renormalized frequency $\tilde{\omega}_{TO}$. Taking the real and imaginary parts of (14), we obtain the TO-phonon shift and width due to the deformation interaction $\zeta(\mathbf{p})$ with carriers:

$$\Delta\omega_k = \text{Re}(\tilde{\omega}_{TO}^2 - \omega_k^2)/2\omega_k, \quad \Gamma = \Gamma^{nat} - \text{Im}\tilde{\omega}_{TO}^2/\omega_k.$$

Second, because of the interaction with carriers, the coupling \tilde{g}_{TO} in (16) has an imaginary part. Therefore,

the line shape of the resonance becomes asymmetric (the Fano resonance),

$$\text{Im } \chi(\mathbf{k}, \omega) = \frac{1}{NM'} \times \frac{\omega \Gamma \tilde{g}_{TO}^2 + (\text{Re } \tilde{\omega}_{TO}^2 - \omega^2) \text{Im } \tilde{g}_{TO}^2}{(\text{Re } \tilde{\omega}_{TO}^2 - \omega^2)^2 + (\omega \Gamma)^2}. \quad (31)$$

The line shape asymmetry depends on the sign of $\text{Re } g_{TO}$. For instance, if $\text{Im } \tilde{g}_{TO}^2 < 0$, the high-frequency wing of the resonance line drops more slowly than the low-frequency one. In the limiting case where $\kappa \gg 1$, we expand

$$\tilde{g}_{TO} = g_{TO} + \frac{\nu_0 \omega}{k} \left\langle \frac{\gamma(\mathbf{p}) \zeta_{TO}(\mathbf{p})}{v} \left(-i\pi + \frac{2\omega}{kv} \right) \delta(\mu) \right\rangle, \quad (32)$$

and for $\kappa \ll 1$ we have

$$\tilde{g}_{TO} = g_{TO} + \frac{\omega \nu_0}{\omega + i\tau^{-1}} \times \left(\langle \gamma(\mathbf{p}) \zeta_{TO}(\mathbf{p}) \rangle + \frac{k^2 \langle v_z^2 \gamma(\mathbf{p}) \zeta_{TO}(\mathbf{p}) \rangle}{(\omega + i\tau^{-1})^2} \right). \quad (33)$$

Notice, that the electron–phonon interaction $\zeta_{TO}(\mathbf{p})$ and the light scattering $\gamma(\mathbf{p})$ by carriers jointly

renormalize the coupling g_{TO} . The frequency renormalization $\tilde{\omega}_{TO}^2$ (see Eq. (14)) results only from the electron–phonon interaction $\zeta_{TO}(\mathbf{p})$. The corresponding expressions can be obtained from Eqs. (32) and (33) by the substitution $\gamma(\mathbf{p}) \rightarrow \zeta_{TO}(\mathbf{p})$. We see that the TO phonons become broader and harder because of the interaction with carriers.

Emphasize that the phonon renormalizations depend on the carrier density ν_0 and the average coupling $\zeta_j(\mathbf{p}) - \langle \zeta_j(\mathbf{p}) \rangle$. They vanish for the isotropic Fermi surface. The maximum value of the relative renormalization has the order of $\lambda a p_F m^* \omega / m |\omega + i\tau^{-1}|$ at $kv \sim |\omega + i\tau^{-1}|$, where λ is the dimensionless electron–phonon coupling and m^* is the effective electron mass.

6.3. The Raman scattering by LO-phonon–plasmon coupled modes

In this case, the carriers interact with each other and the ion vibrations via both the macroscopic electric field $E(\mathbf{r}, t)$ and the deformation potential $\zeta_{LO}(\mathbf{p})$. In the long-wave limit $k \rightarrow 0$, Eqs. (15), (20), and (21) show no renormalization of the ionic charge, $\tilde{Z} = \bar{Z} = Z$, and of the electro-optic constant, $\tilde{g}_E = g_E$. Equation (23) then becomes

$$\chi(0, \omega) = \chi_e(0, \omega) + \frac{\tilde{g}_{LO}^2 \varepsilon_e(0, \omega) / NM' - 4\pi g_E^2 (\tilde{\omega}_0^2 - i\omega \Gamma^{nat} - \omega^2) - 8\pi g_E \tilde{g}_{LO} Z / M'}{(\tilde{\omega}_0^2 - i\omega \Gamma^{nat} - \omega^2) \varepsilon_e(0, \omega) + 4\pi N Z^2 / M'}, \quad (34)$$

where the first term is given in Eq. (28). The deformation potential $\zeta_{LO}(\mathbf{p})$ renormalizes the phonon frequency $\tilde{\omega}_0$ in (14), as well as the deformation-optic constant \tilde{g}_{LO} in (16). The corresponding expansions in the limiting cases are similar to Eqs. (32) and (33). All mentioned above about the TO line asymmetry also applies to the LO line.

Because the dielectric function of the electron–ion system is given by

$$\varepsilon(0, \omega) = \varepsilon_e(0, \omega) + \frac{4\pi N Z^2}{M' (\tilde{\omega}_0^2 - i\omega \Gamma^{nat} - \omega^2)}, \quad (35)$$

the second term in the right-hand side of Eq. (34) has poles at the points where $\varepsilon(0, \omega) = 0$. This condition defines the frequency of coupled phonon–plasmon modes in the long-wave limit.

In the absence of the electron and phonon collisions ($\tau^{-1} = \Gamma^{nat} = 0$), and without the electron–phonon interaction ($\zeta(\mathbf{p}) = 0$), we obtain a biquadratic equation using Eq. (29). It gives the frequencies of the coupled phonon–plasmon modes at $k = 0$,

$$\omega_{\pm}^2 = \frac{1}{2} (\omega_{pe}^2 + \omega_{LO}^2) \pm \frac{1}{2} [(\omega_{pe}^2 + \omega_{LO}^2)^2 - 4\omega_{pe}^2 \omega_{TO}^2]^{1/2}, \quad (36)$$

where $\omega_{TO} = \omega_k$ is the TO-mode frequency at $k = 0$, $\omega_{LO}^2 = \omega_{TO}^2 + \omega_{pi}^2$, and $\omega_{pi}^2 = 4\pi N Z^2 / \varepsilon_{\infty} M'$. These frequencies (related to ω_{TO}) are shown in Fig. 1 as functions of the electron concentration, namely, $\omega_{pe} / \omega_{TO}$. The upper line begins at ω_{LO} and tends to the electron plasma frequency ω_{pe} . The lower frequency starts as $\omega_{pe} \omega_{TO} / \omega_{LO}$ and then approaches ω_{TO} . In other words, observing the longitudinal phonon mode in the optic range and adding electrons, we see a transition of the longitudinal phonon frequency from ω_{LO} to ω_{TO} . This is a result of the Coulomb screening.

We can compare Eq. (34) with the theory of Hon and Faust [11]. Because the electron–phonon interaction, $\zeta_{LO}(\mathbf{p})$, as well as the electronic scattering, $\gamma(\mathbf{p})$, were ignored in their theory, the phonon frequency and the deformation-optic constant were not renormalized. Equation (34) can then be rewritten as

$$\chi(0, \omega) = \frac{(4\pi g_E)^2}{\varepsilon_\infty \varepsilon(0, \omega)} \times \left[\frac{\varepsilon_e(0, \omega)}{\varepsilon_\infty} A^2 \chi_I - \frac{\varepsilon_\infty}{4\pi} - 2A \chi_I \right], \quad (37)$$

where

$$\chi_I = NZ^2/M'(\omega_{TO}^2 - i\omega\Gamma^{nat} - \omega^2),$$

$$A = \frac{C\omega_{TO}^2 M' \varepsilon_\infty}{4\pi N Z^2}, \quad C = \frac{g_{LO} Z}{g_E M \omega_{TO}^2},$$

C is the Faust–Henry coefficient. We now see that expression (37) coincides with the result of Hon and Faust (see, e.g. Eq. (3.1) in [13]).

For $k \neq 0$, Eq. (23), first, includes the dielectric function (19) that differs from the Lindhard–Mermin expression. Second, the condition determining frequencies and damping of the phonon–plasmon coupled modes,

$$(\tilde{\omega}_j^2 - i\omega\Gamma^{nat} - \omega^2)\varepsilon_e(\mathbf{k}, \omega) + 4\pi N \tilde{Z} \bar{Z}/M' = 0, \quad (38)$$

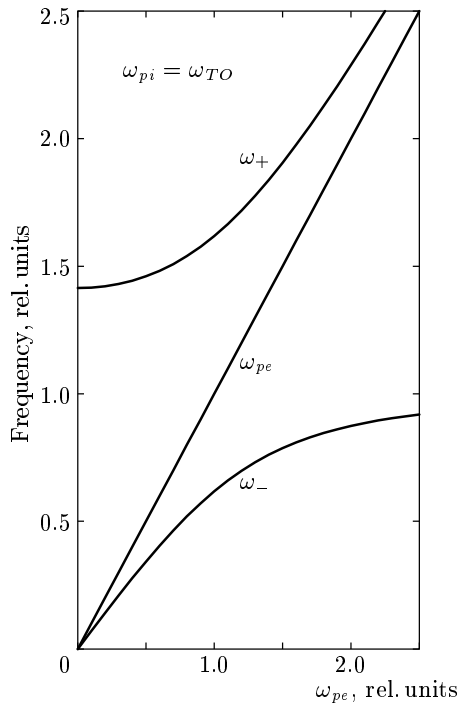


Fig. 1. Frequencies (in units of ω_{TO}) of the phonon–plasmon modes at $k = 0$ versus the free-carrier concentration, namely, the electron plasma frequency (in units of ω_{TO}). We set the ion plasma frequency $\omega_{pi} = \omega_{TO}$ in the absence of the free carriers. Then

$$\omega_{LO}/\omega_{TO} = \sqrt{2}$$

contains the phonon frequency $\tilde{\omega}$ and the ionic charge renormalized by the electron–phonon interaction $\zeta_{LO}(\mathbf{p})$. Third, the electro-optic coupling g_E in Eq. (21) is modified because of the light scattering $\gamma(\mathbf{p})$ from the electron–hole pairs. This effect is not canceled in the product $g_{LO}\tilde{g}_E$ in Eq. (23) even in the absence of the electron–phonon interaction $\zeta_{LO}(\mathbf{p})$. The expansion of \tilde{g}_E has the form

$$\tilde{g}_E = g_E - \frac{ie\nu_0 k \langle v_z^2 \gamma(\mathbf{p}) \rangle}{(\omega + i\tau^{-1})^2} \quad (39)$$

for $|\kappa| \ll 1$ and

$$\tilde{g}_E = g_E + e\nu_0 k^{-2}(\omega + i\tau^{-1}) \times \left\langle \frac{\gamma(\mathbf{p})}{v} \left(-\frac{\pi}{2} - \frac{i\omega}{kv} \right) \delta(\mu) \right\rangle \quad (40)$$

for $|\kappa| \gg 1$. We note that the term $\tilde{g}_{LO}\bar{g}_E$ has the largest imaginary part for $\omega\tau \approx 1$ and then results most significantly in the line shape asymmetry.

Schematically, the dispersion of the phonon–plasmon modes is shown in Fig. 2. There are two main peculiarities in this figure. First, the behavior of the upper mode near the line $\omega = kv_F$. Around this line ($\tau^{-1} < \omega - kv_F \ll kv_F$), dielectric function (19) has a singularity,

$$\varepsilon_e(k, \omega) = \varepsilon_\infty + \varepsilon_\infty \frac{k_0^2}{k^2} \left\{ 1 - \frac{\omega}{2kv_F} \times \left[\frac{1}{2} \ln \frac{4k^2 v_F^2}{(\omega - kv_F)^2 + \tau^{-2}} - i \frac{\tau^{-1}}{\omega - kv_F} \right] \right\}. \quad (41)$$

Because of this singularity, the upper mode approaches the asymptote $\omega = kv_F$ as the wave vector k increases. Second, in the region $kv_F \gg \omega$, there is always one mode that has a predominantly phonon character. The reason is the decrease with k of the imaginary part of dielectric function (26).

7. DISCUSSION

We now consider the obtained results in a simplest way. We assume that the electronic scattering is negligibly small, $\gamma(\mathbf{p}) = 0$. The second term in the parentheses in Eq. (14) is less than the first one in both limiting cases, $\kappa \ll 1$ and $\kappa \gg 1$. We neglect this term at all. We also do not take the ion charge renormalization into account because it vanishes at small values of κ . We can then use expression (25) not only for the dielectric function $\varepsilon_e(\mathbf{k}, \omega)$, Eq. (19), but also for the renormalized phonon frequency $\tilde{\omega}$, Eq. (14).

In such an approximation, solving Eq. (38), we find the frequency and damping of the phonon-like mode for the limiting cases of the parameter $\kappa = kv_F/(\omega + i/\tau)$ and for low and large carrier concentration.

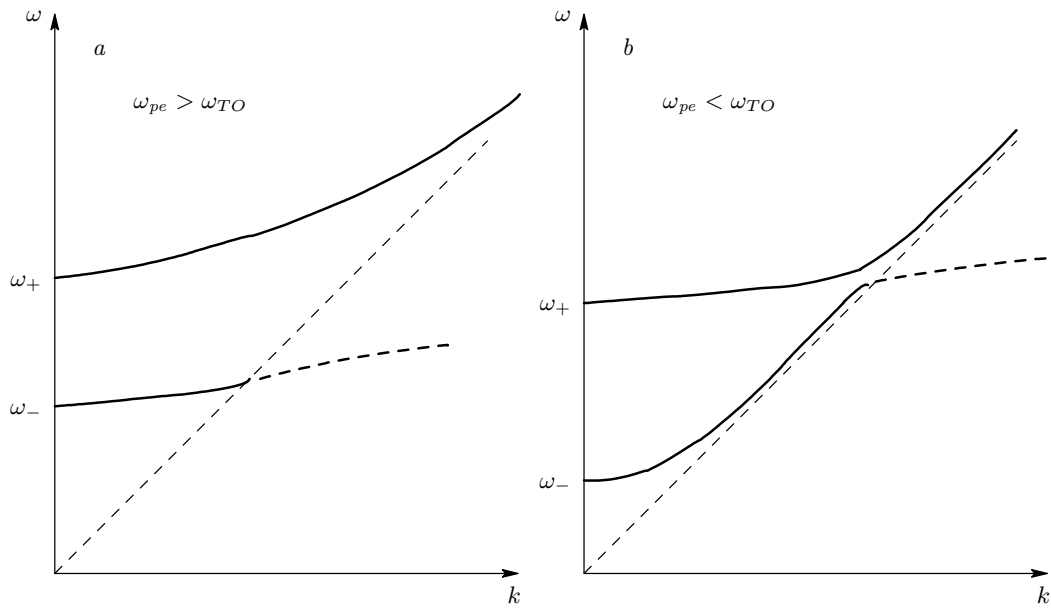


Fig. 2. Schematic representation of the dispersion of phonon–plasmon modes (a) for metallic ($\omega_{pe} > \omega_{TO}$) and (b) for semiconducting ($\omega_{pe} < \omega_{TO}$) carrier concentrations. The dashed straight lines separate the domain $kv_F > \omega$ where the Landau damping exists; the dashed curves represent damped modes there

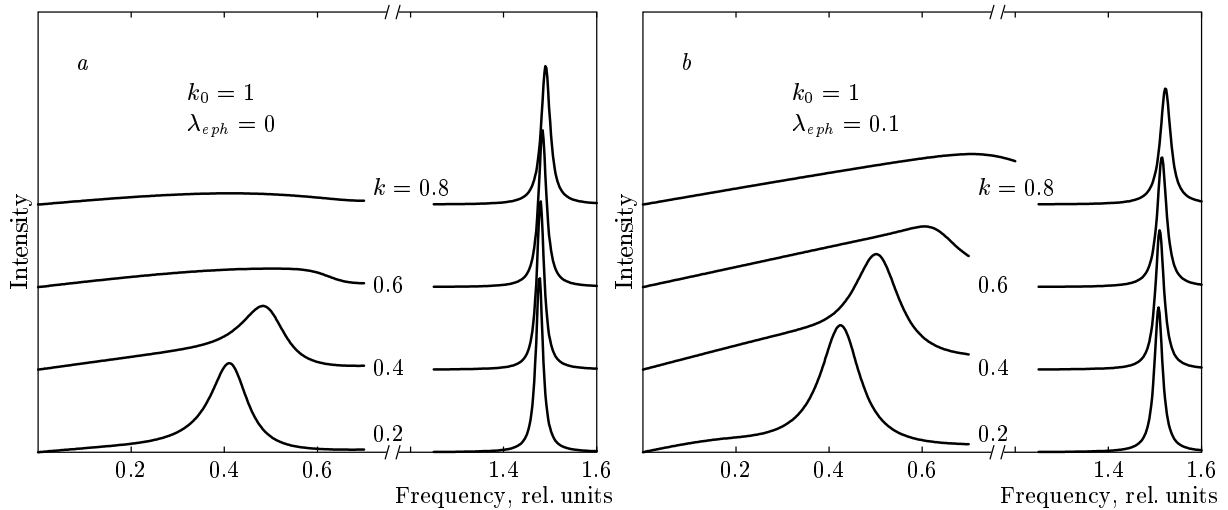


Fig. 3. Raman spectra from a semiconductor with low carrier concentration as a function of the frequency transfer ω for the indicated values of the momentum transfer k , the Thomas–Fermi parameter k_0 (in units of ω_{TO}/v_F), and the electron–phonon coupling constant $\lambda_{eph} = 0$ (a) and $\lambda_{eph} = 0.1$ (b). We set the ion plasma frequency $\omega_{pi} = \omega_{TO}$, the phonon natural width $\Gamma^{nat}/\omega_{TO} = 10^{-2}$, and the carrier relaxation rate $\tau^{-1}/\Gamma^{nat} = 10$

1) Low carrier concentration, $\omega_{pe} < \omega_O$:
 $|\kappa| \ll 1$,

$$\omega^2 = \omega_{LO}^2 - i\omega\Gamma^{nat} + \frac{\lambda_{eph}\omega\omega_{TO}^2}{\omega^*} \left(1 + \frac{\kappa^2}{3}\right) + \frac{(\omega_{pi}\omega_{pe})^2}{\omega\omega^*} \left(1 + \frac{i\kappa^2}{3\omega\tau}\right);$$

$$|\kappa| \gg 1,$$

$$\omega^2 = \omega_{LO}^2 - i\omega\Gamma^{nat} + \frac{\lambda_{eph}\omega\omega_{TO}^2}{kv_F} \left(-i\frac{\pi}{2} + \frac{1}{\kappa}\right) - \frac{3(\omega_{pi}\omega_{pe})^2}{(kv_F)^2} \left(1 + \frac{i\pi\omega}{2kv_F}\right),$$

where $\omega^* = \omega + i/\tau$ and instead of ω we must substitute $\omega \rightarrow \omega_{LO}$.

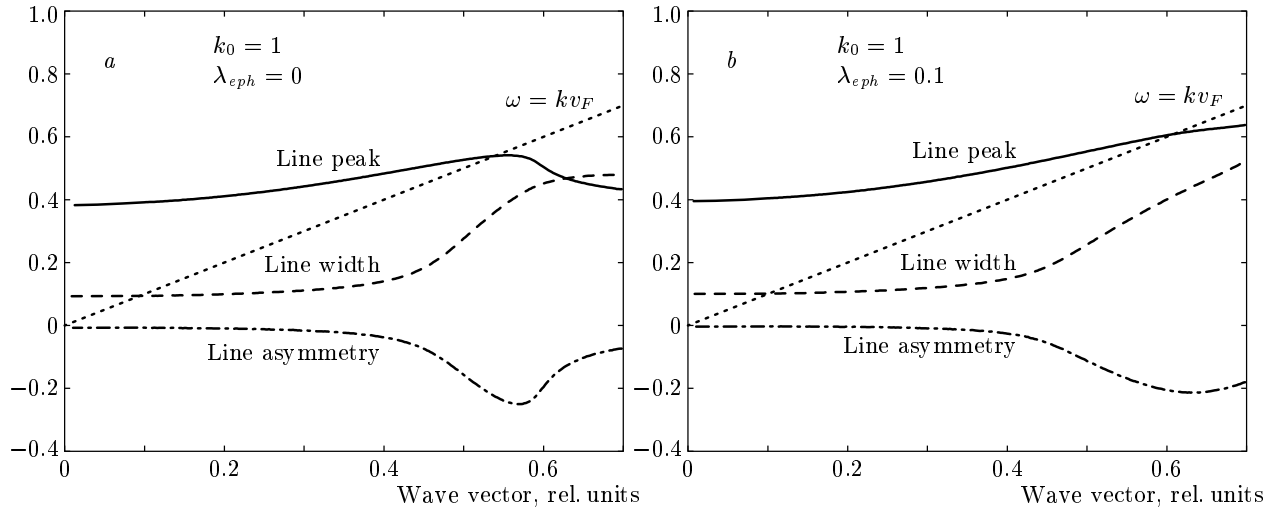


Fig. 4. The plasmon dispersion as a function of k in units of ω_{TO}/v_F (the position in units of ω_{TO} of the line peak of Raman spectra; upper part of the figure, solid line) for $k_0 = 1$ and $\lambda_{eph} = 0$ (a) and $\lambda_{eph} = 0.1$ (b). In the bottom, the line width (the full width at half maximum, dashed line) and the line asymmetry (the difference between the right and left wings at half maximum, dash-dotted line) in units of ω_{TO} . The Landau damping exists to the right of the dotted line $\omega = kv_F$

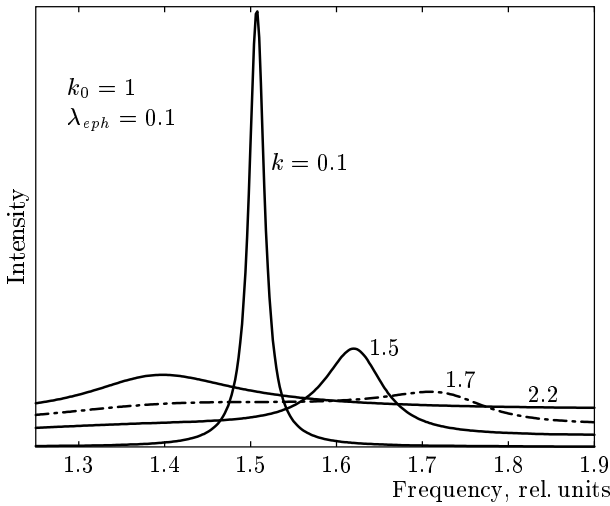


Fig. 5. The LO phonon Raman spectra for large momentum transfers k

2) Large carrier concentration, $\omega_{pe} \gg \omega_{TO}$:

$$|\kappa| \ll 1,$$

$$\omega^2 = \omega_{TO}^2 - i\omega\Gamma^{nat} + \frac{\lambda_{eph}\omega\omega_{TO}^2}{\omega^*} \left(1 + \frac{\kappa^2}{3}\right) - \frac{\omega_{pi}^2\omega\omega^*}{\omega_{pe}^2} \left(1 - \frac{i\kappa^2}{3\omega\tau}\right);$$

$$|\kappa| \gg 1,$$

$$\omega^2 = \omega_{TO}^2 - i\omega\Gamma^{nat} + \frac{\lambda_{eph}\omega\omega_{TO}^2}{kv_F} \left(-i\frac{\pi}{2} + \frac{1}{\kappa}\right) + \frac{(\omega_{pi}kv_F)^2}{3\omega_{pe}^2} \left(1 - \frac{i\pi\omega}{2kv_F}\right),$$

where we substitute $\omega \rightarrow \omega_{TO}$. The definition of λ_{eph} depends on κ ,

$$\lambda_{eph} = \frac{\nu_0 \langle \zeta^2(\mathbf{p}) \rangle}{M'N\omega_{TO}^2}, \quad \kappa \ll 1,$$

$$\lambda_{eph} = \frac{\nu_0 v_F^2 \langle \zeta^2(\mathbf{p})/v_z^2 \rangle}{M'N\omega_{TO}^2}, \quad \kappa \gg 1,$$

but gives the same order of value, $\lambda_{eph} \sim p_F am^*/m$.

Results of the numerical calculations of the Raman spectra, Eq. (23), in this approximation are shown in Fig. 3 for two values of the electron–phonon coupling λ_{eph} . We take the value of the Faust–Henry coefficient $C = -0.5$ and the phonon natural width $\Gamma^{nat} = 10^{-2}\omega_{TO}$. The electron collision rate is taken as $\tau^{-1} = 10^{-1}\omega_{TO}$, which is the usual value for heavily doped semiconductors [13, 19]. In Fig. 3, the wave vector k and the Thomas–Fermi parameter k_0 are given in units of ω_{TO}/v_F , and the frequency ω in units of ω_{TO} . Both these figures correspond to the case of small carrier numbers $\omega_{pe} < \omega_{TO}$ (see Fig. 2b; for the quadratic electron spectrum, $\omega_{pe} = k_0 v_F/\sqrt{3}$). The left peak mainly has a plasmon character and the right peak is mainly the LO phonon. We put the ion plasmon frequency $\omega_{pi} = \omega_{TO}$, therefore $\omega_{LO} = \sqrt{2}\omega_{TO}$. As the

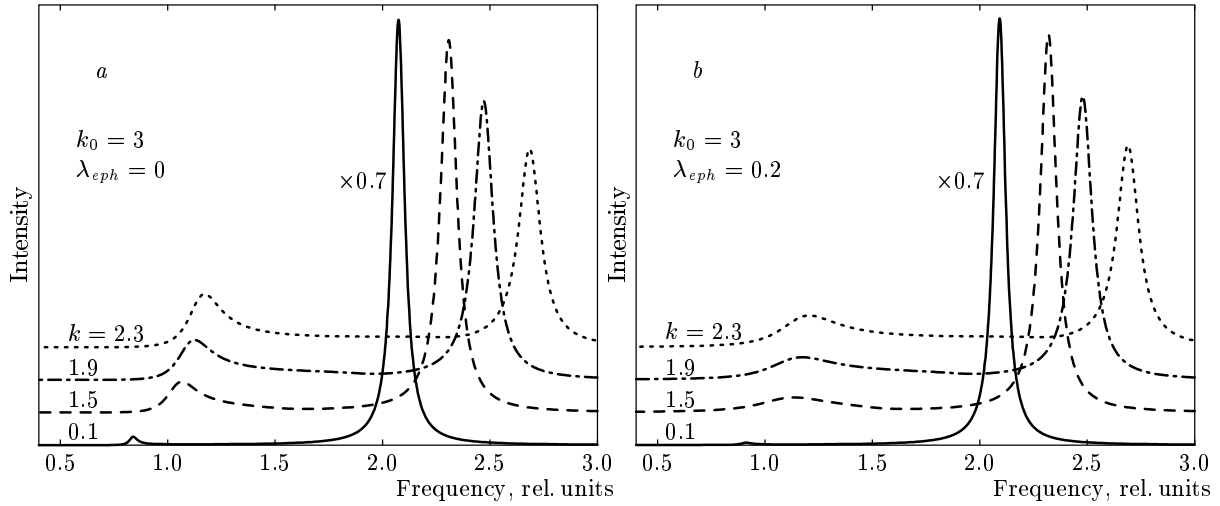


Fig. 6. Raman spectra from a heavily doped semiconductor for $k_0 = 3$ and $\lambda_{eph} = 0$ (a) and $\lambda_{eph} = 0.2$ (b); the notations as in Fig. 1

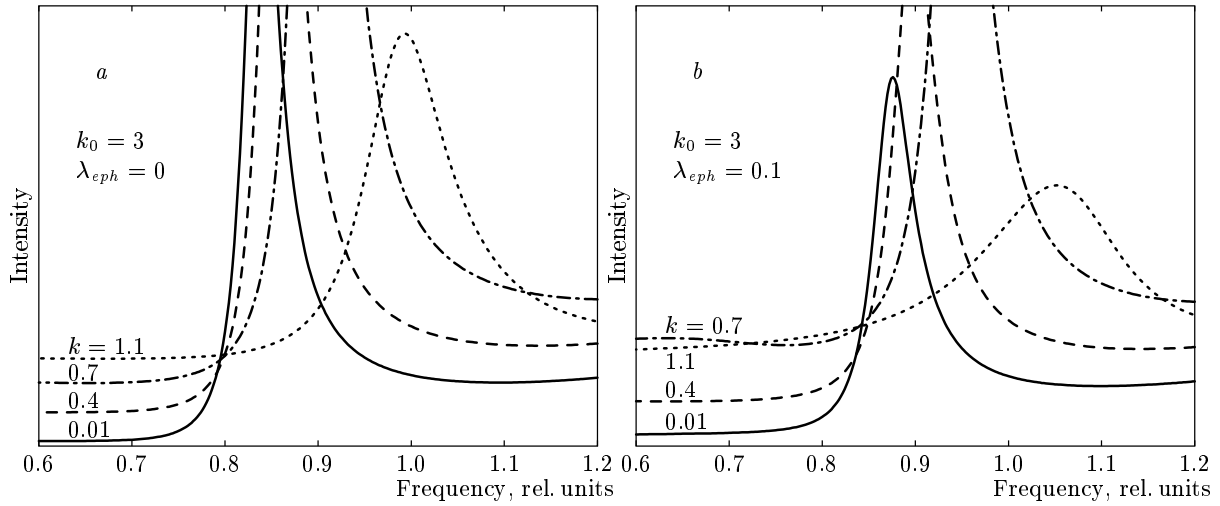


Fig. 7. The LO phonon part of the Raman spectra from heavily doped semiconductor for various momentum transfers without (a) and with (b) electron-phonon interaction taken into account

wave vector k approaches the boundary of the Landau damping region $kv_F > \omega$, the plasmon peak becomes broader and almost disappears at $k = 0.8$. The broad continuum in the region $kv_F > \omega$ results from the excitation of electron-hole pairs. The intensity of the plasmon peak becomes larger in comparison to the phonon peak as the electron-phonon interaction λ_{eph} increases.

The k -dispersion of the plasmon (the peak position of the Raman spectra as a function of k), the line width (the full width at half maximum), and the line asymmetry (the frequency difference between the right and left wings of the resonance line at half maximum) are shown in Fig. 4, all in units of ω_{TO} . The width

and asymmetry become much larger while the plasmon peak is immersed in the electron-hole continuum. The maximum in this region of the spectra is nothing but the electron-hole contribution. In Fig. 4b, we see how close this maximum is located to the line $\omega = kv_F$ for $\lambda_{eph} = 0.1$.

The behavior of the phonon peak around $\omega = \omega_{LO}$ as k increases is shown in Fig. 5. As the wave vector increases from $k = 0$ to $k = 1.7$, the phonon peak is evidently shifted to the higher frequency and becomes broader. This is an effect of the Landau damping (see Fig. 2b). But for $k > 1.75$, this peak appears at a lower frequency, $\omega \approx 1.4$, and becomes sharper for

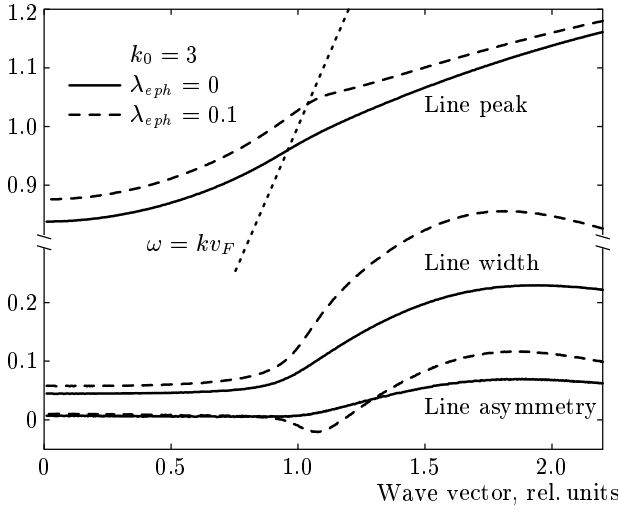


Fig. 8. Dispersion of the phonon peak (upper), the line width, and the line asymmetry (bottom). The boundary of the Landau damping region is shown with a dotted line

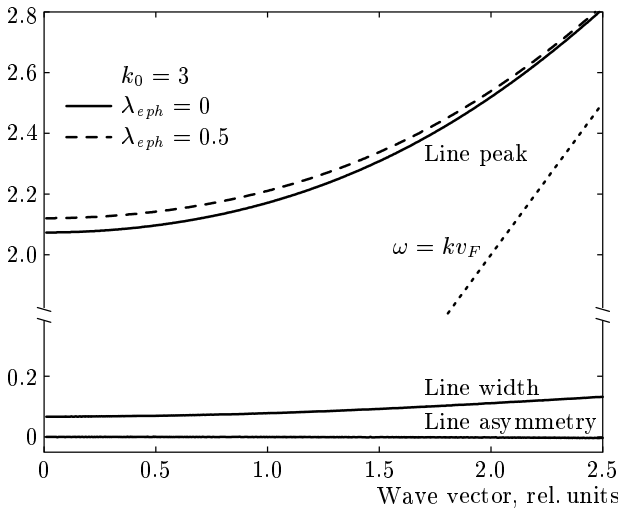


Fig. 9. Dispersion of the plasmon peak in heavily doped semiconductors

$k > 2.2$ because the Landau damping decreases with k (see Eq. (26)).

The Raman spectra for heavily doped semiconductors and metals are shown in Fig. 6 (see also Fig. 2a). The phonon peak is now located around $\omega \sim \omega_{TO}$ instead of $\omega \sim \omega_{LO}$. This is an effect of the Coulomb screening: carriers decrease the frequency of the LO mode from ω_{LO} to ω_{TO} . We also see that the electron-phonon interaction suppresses the phonon peak.

The effect of the Coulomb screening and the elect-

ron-phonon interaction on the phonon mode is clearly seen in Fig. 7, where the phonon part of the spectra is shown in detail. The lines are very asymmetric. The phonon dispersion, the line width, and the line asymmetry as functions of k are shown in Fig. 8. We see a singularity at $k \approx \omega/v_F$. It is interesting to estimate the value of the phonon dispersion. With the help of Fig. 7b, we find $d\omega/dk \leq 10^{-1}v_F$. On the other hand, using Eqs. (26) and (29), we find for the phonon dispersion $\omega^2 = \omega_{TO}^2 + \omega_{pi}^2 k^2/k_0^2$, which corresponds well with the previous estimate for our values of k_0 and ω_{pi} . We note that these estimates confirm the adiabatic approximation, because the value of dispersion $s = \omega_{pi}/k_0 \sim v_F \sqrt{m/M}$ contains the adiabatic parameter.

In Fig. 9, the dispersion, the line width, and the line asymmetry are shown for the plasmon peak in heavily doped semiconductors. Here, the effect of the electron-phonon interaction on the phonon dispersion is weak and no influence on the width and asymmetry of the line is seen.

8. CONCLUSIONS

In conclusion, we first emphasize that our result (23) describes the renormalization of the phonon frequencies, the effective ion charge, and the coupling constants due to the electron-phonon deformation interaction $\zeta_j(\mathbf{p})$. Second, this result involves the k -dependent semiclassical dielectric function instead of the Lindhard-Mermin expression. Finally, the light scattering vertex $\gamma(\mathbf{p})$ with excitations of the electron-hole pairs not only gives an additional contribution χ_e in Eq. (23), but also modifies the electro-optic g_E and deformation-optic g_j coupling constants, which become dependent on the frequency and momentum transfers.

The author acknowledges the kind hospitality of the Max-Planck-Institut für Physik komplexer Systeme (Dresden), where this work was completed. The work was partially supported by the RFBR (grant № 01-02-16211).

REFERENCES

1. A. B. Migdal, Zh. Eksp. Teor. Fiz. **34**, 1438 (1958) [Sov. Phys. JETP **7**, 996 (1958)].
2. A. A. Abrikosov, L. P. Gor'kov, and I. Ye. Dzyaloshinskii, *Methods of Quantum Field Theory in Statistical Physics*, Prentice-Hall, Englewood Cliffs, NJ (1963).

3. A. S. Alexandrov and J. R. Schrieffer, *Phys. Rev. B* **56**, 13731 (1997).
4. M. Born and Kung Huang, *Dynamical Theory of Crystal Lattices*, Oxford University Press, New York (1954).
5. E. G. Brovman and Yu. Kagan, *Zh. Eksp. Teor. Fiz.* **52**, 557 (1967) [*Sov. Phys. JETP* **25**, 365 (1967)].
6. V. M. Kontorovich, *Usp. Fiz. Nauk* **142**, 265 (1984) [*Sov. Phys. Uspekhi* **27**, 134 (1984)].
7. M. Reizer, *Phys. Rev. B* **61**, 40 (2000).
8. V. L. Gurevich, A. I. Larkin, and Yu. A. Firsov, *Fiz. Tv. Tela* **4**, 185 (1962).
9. L. A. Falkovsky, *Phys. Rev. B* **66**, 020302-1 (2002); *Zh. Eksp. Teor. Fiz.* **122**, 411 (2002) [*JETP* **95**, 354 (2002)].
10. G. Abstreiter, M. Cardona, and A. Pinczuk, *Light Scattering in Solids*, Topics in Applied Physics, Vol. 54, ed. by M. Cardona and G. Güntherodt, Springer, Berlin (1984), p. 5.
11. D.T. Hon and W. L. Faust, *Appl. Phys.* **1**, 241 (1973).
12. B. H. Bairamov, I. P. Ipatova, V. A. Milorava, V. V. Toporov, K. Naukkarinen, T. Tuomi, G. Irmer, and J. Monecke, *Phys. Rev. B* **38**, 5722 (1988).
13. L. Artús, R. Cuscó, and J. Ibáñez, *Phys. Rev. B* **60**, 5456 (1999).
14. N. D. Mermin, *Phys. Rev. B* **1**, 2362 (1970).
15. L. A. Falkovsky and E. G. Mishchenko, *Phys. Rev. B* **51**, 7239 (1995).
16. A. A. Abrikosov and V. M. Genkin, *Zh. Eksp. Teor. Fiz.* **65**, 842 (1974) [*Sov. Phys. JETP* **38**, 417 (1974)].
17. A. A. Abrikosov and L. A. Falkovsky, *Zh. Eksp. Teor. Fiz.* **40**, 262 (1961) [*Sov. Phys. JETP* **13**, 179 (1961)].
18. A. Zawadowski and M. Cardona, *Phys. Rev. B* **42**, 10732 (1990).
19. R. Fukasawa and S. Perkowitz, *Phys. Rev. B* **50**, 14119 (1994).